



Hopping-induced quantum phase transition in the Ising-Rabi lattice model

Gaoke Hu ^{1,2} Zhiguo Lü ^{3,*} Haiqing Lin,⁴ and Hang Zheng^{2,3,†}

¹*School of Systems Science/Institute of Nonequilibrium Systems, Beijing Normal University, Beijing 100875, China*

²*Beijing Computational Science Research Center, Beijing 100193, China*

³*Key Laboratory of Artificial Structures and Quantum Control (Ministry of Education), School of Physics and Astronomy, Shanghai Jiao Tong University, Shanghai 200240, China*

⁴*School of Physics, Zhejiang University, Hangzhou 310058, China*



(Received 9 January 2023; accepted 8 August 2023; published 23 August 2023)

We study the ground state and low-lying polaritonic excitation states in the Ising-Rabi lattice model (IRLM), where the transverse field in the quantum transverse field Ising model is replaced by a quantized local photon field. The competition among the photon-hopping coupling, the intrasite Rabi interaction, and the Ising interaction drives the system across a quantum phase transition from the insulating phase to the delocalized superradiant phase. Mean-field theory confirms the existence of the quantum phase transition and the analytical expressions for the phase boundary are derived. The spectra of low-lying polaritonic excitations and Bose-Einstein condensation are further explored by a unitary transformation method. The deep strong-coupling analysis reveals a quantum criticality, where the IRLM belongs to the universality class of the XYZ model. When the hopping strength $t = 0$, the properties of the ground state in the IRLM are investigated by the symmetry analysis and the density-matrix renormalization-group method. It turns out that the photon field cannot alone serve as a global transverse field in the quantum transverse field Ising model without the presence of hopping coupling since a crossover behavior instead of a quantum phase transition is confirmed.

DOI: [10.1103/PhysRevA.108.023723](https://doi.org/10.1103/PhysRevA.108.023723)

I. INTRODUCTION

The light-matter interaction processes are fundamental to understand our nature and lie at the center of various quantum technologies, including lasers and many quantum computing architectures [1–3]. Traditionally, the light-matter process has been studied in an optical cavity, where the electromagnetic radiation can be confined in a cavity and repeatedly absorbed and emitted by an embedded atom, which is known as cavity quantum electrodynamics [4,5]. In the simplest case, the electromagnetic radiation specified by a single-mode quantum field interacts with a two-level atom, which is referred to as the Rabi model [6]. In the standard cavity quantum electrodynamics experiments, when the coherent energy exchange is comparable or larger than the rate of dissipation in the material, the system is in the strong-coupling regime [7,8]. In this regime, one of the useful approximations is the rotating-wave approximation (RWA), i.e., the neglect of the counter-rotating coupling (CRC) terms, and the Rabi model reduces to the Jaynes-Cummings model [9]. In the past decade, both in theoretical insights and experimental achievements [10–12], the physics of light-matter interaction in ultrastrong-coupling regime are explored, where the rate between the coupling strength and photon frequency reaches $g/\omega \gtrsim 0.1$. In the ultrastrong-coupling regime, RWA is not valid anymore and the CRC terms lead to novel features,

such as the Bloch-Siegert shift [13,14]. Recently, the deep strong-coupling (DSC) regime has been transitioned from a theoretical study to an experimental reality [15–17], where the rate $g/\omega \gtrsim 1$.

With the fast development of technology, quantum simulators pave the way for realizing light-matter coupling systems in the array of optical lattices to understand the emergent phenomena in strongly correlated many-body systems. Compared with the traditional strongly interacting condensed-matter systems, the quantum optical systems have relatively large distances and timescales, which allow for the high level of the measurement and manipulation of individual cavities at the quantum level [18,19]. In quantum simulator systems, the interaction among the different sites can be described by the hopping term [20–22], which compete with the on-site coupling and give rise to rich physical phenomena. For example, an experimental realization of the Rabi lattice model (RLM) using trapped ions is reported and its equilibrium properties and quantum dynamics are controllably studied [23]. With different types of hopping coupling, different sites couple together by tunneling of photons, and a variety of novel phases are demonstrated in the RLM. For the negative hopping coupling, the RLM undergoes the quantum phase transition from the insulating phase to the delocalized superradiant phase [24–26]. Due to the CRC terms breaking the conservation polariton number, the Mott's lobes are absent in the phase diagram of the RLM [24–28]. When neighboring sites are coupled by positive hopping interaction, the frustrated superradiant phase transition is reported on a triangle motif [29]. Besides, the complex photon-hopping coupling with a phase

*zgly@sjtu.edu.cn

†hzheng@sjtu.edu.cn

can be induced by an artificial magnetic field, which leads to the breaking of the time-reversal symmetry and a chiral superradiant phase can emerge in the quantum Rabi ring [30–32]. We notice that in all of those systems the photon fields couple with the localized two-level systems. We are thus motivated to explore the physics in a general light-matter system, where the photon field couples with the strongly correlated model inherently.

The quantum transverse field Ising (QTFI) model is one of the simplest paradigmatic strongly correlated models [33], which reads as

$$\hat{H}_{\text{TI}} = h \sum_i \hat{\sigma}_i^x - J \sum_{\langle i,j \rangle} \hat{\sigma}_i^z \hat{\sigma}_j^z, \quad (1)$$

where h is the strength of the external transverse field and J is the Ising interaction strength between nearest-neighbor sites. In the experiments [34,35], the QTFI model can couple with the photon field inherently, through replacing the tunable transverse field h by a quantized photon field, i.e., $(\hat{b}_i^\dagger + \hat{b}_i)$, for example, one mode of a cavity in each site. After this substitution, the system is described by the Hamiltonian of the Ising-Rabi lattice model (IRLM) in the following:

$$\begin{aligned} \hat{H}_{\text{IR}} = & \sum_i \omega \hat{b}_i^\dagger \hat{b}_i + \sum_i g \hat{\sigma}_i^x (\hat{b}_i^\dagger + \hat{b}_i) - J \sum_{\langle i,j \rangle} \hat{\sigma}_i^z \hat{\sigma}_j^z \\ & - t \sum_{\langle i,j \rangle} (\hat{b}_i^\dagger \hat{b}_j + \hat{b}_i \hat{b}_j^\dagger), \end{aligned} \quad (2)$$

where g is the strength of the Rabi interaction, and \hat{b}_i^\dagger (\hat{b}_i) is the creation (annihilation) operator of a single-mode cavity with the frequency ω . The corresponding hopping of photons between nearest-neighbor cavities is described by the last term in Eq. (2), i.e., $-t(\hat{b}_i^\dagger \hat{b}_j + \hat{b}_i \hat{b}_j^\dagger)$, with the parametrized coupling strength t . In this model, the photon field of the IRLM inherently couples with the strongly correlated Ising model. As the schematic of the IRLM shown in Fig. 1, nearest-neighbor sites are simultaneously coupled by the Ising interaction and photon-hopping coupling. The IRLM can be realized by the trapped-ion setups [34,35], where hopping coupling comes from the Coulomb interaction between ions [20–22]. When the photon-hopping coupling terms are neglected, the model is reduced to the one in Ref. [35]. The Hamiltonian of the IRLM has the discrete global \mathbb{Z}_2 symmetry, with the parity operator $\hat{P} = \prod_i^N \exp[i\pi(\hat{b}_i^\dagger \hat{b}_i + \hat{\sigma}_i^+ \hat{\sigma}_i^-)]$.

In this paper, we demonstrate that the competition among the photon-hopping coupling, the intrasite Rabi interaction and the Ising interaction drives the system across a quantum phase transition from the insulating phase to the delocalized superradiant phase. We use mean-field theory (MFT) to calculate the phase diagram and the unitary transformation method to calculate the spectra of lower-energy excitations and further elucidate the Bose-Einstein condensation. The DSC analysis reveals a quantum criticality, where the IRLM belongs to the universality class of the XYZ model. We compare the cases with the finite hopping coupling ($t \neq 0$) with those with vanishing hopping coupling ($t = 0$). In the finite hopping coupling case, positive critical hopping strengths are obtained. When the hopping strength $t = 0$, both the symmetry analysis

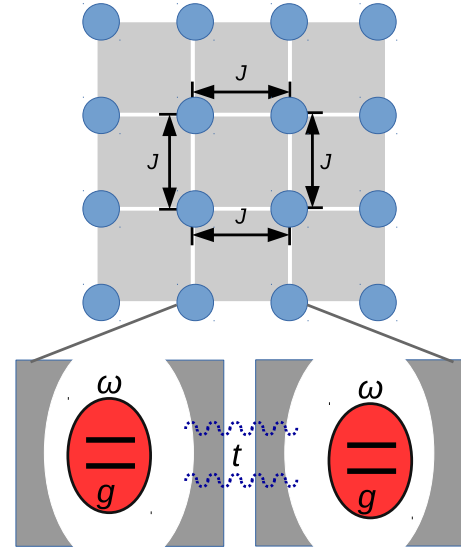


FIG. 1. Schematic of the Ising-Rabi lattice model (IRLM) in a two-dimensional square lattice. Nearest-neighbor sites are coupled simultaneously by the Ising interaction with strength J and photon-hopping coupling with strength t .

and the density-matrix renormalization group (DMRG) results display a crossover behavior instead of a quantum phase transition as the Ising interaction increases. The comparison demonstrates the necessity of the photon-hopping coupling for inducing the quantum phase transition. Despite the fact that the IRLM stems from the QTFI, we prove that the photon field alone cannot serve as a global transverse field without the presence of hopping coupling.

This paper is organized as follows: The mean-field treatment is applied on the IRLM in Sec. II, where we provide analytical expressions for the phase boundary. The correspondence beyond the mean-field level is explored in Sec. III, where we introduce the unitary transformations to study polaritonic excitations behavior in the IRLM. In Sec. III A, the ground states and polaritonic excitation spectra in the insulating phase are calculated. The DSC limit is considered in Sec. III B. In Sec. III C, the polaritonic excitation spectra and the order parameter in the delocalized superradiant phase are presented. In Sec. IV, the ground-state properties of the IRLM in the case of $t = 0$ are explored by the symmetry analysis and the DMRG. Finally, we give the conclusion of the present work in Sec. V.

II. MEAN-FIELD THEORY

The main idea in MFT is that it neglects the correlations between different sites, then the photon-hopping coupling terms and Ising interaction in the IRLM are decoupled as

$$\hat{b}_i^\dagger \hat{b}_j \simeq \langle \hat{b}_i^\dagger \rangle \hat{b}_j + \hat{b}_i^\dagger \langle \hat{b}_j \rangle - \langle \hat{b}_i^\dagger \rangle \langle \hat{b}_j \rangle, \quad (3)$$

$$\hat{\sigma}_i^z \hat{\sigma}_j^z \simeq \langle \hat{\sigma}_i^z \rangle \hat{\sigma}_j^z + \hat{\sigma}_i^z \langle \hat{\sigma}_j^z \rangle - \langle \hat{\sigma}_i^z \rangle \langle \hat{\sigma}_j^z \rangle. \quad (4)$$

Here, we introduce the order parameter $\psi \equiv \langle \hat{b}_j \rangle$. The expectation value of $\hat{\sigma}_i^z$ in the ground state is noted as $m = -\langle \hat{\sigma}_i^z \rangle$. Then, the original IRLM Hamiltonian [Eq. (2)] reduces to a

mean-field Hamiltonian, namely

$$\hat{H}_{\text{MF}} = \sum_i zJm\hat{\sigma}_i^z + \omega\hat{b}_i^\dagger\hat{b}_i + g\hat{\sigma}_i^x(\hat{b}_i^\dagger + \hat{b}_i) - zt\psi(\hat{b}_i^\dagger + \hat{b}_i) + ztN\psi^2 + \frac{zJm^2N}{2}, \quad (5)$$

where z is the coordination number. The order parameter is determined by minimizing the ground-state energy of the mean-field Hamiltonian, and the parameter m can be determined self-consistently. When $\psi = 0$ reveals an insulating phase (or a disordered phase), characterized by the fixed parity number with respect to \hat{P} , $\langle\hat{b}_i\rangle = 0$ and $\langle\hat{\sigma}_i^x\rangle = 0$. Above the critical photon-hopping strength t_c , a symmetry-breaking long-range ordering phase emerges, where the photon field becomes coherent $\langle\hat{b}_i\rangle \neq 0$, and the two-level atoms polarize to generate a ferroelectrically ordered state $\langle\hat{\sigma}_i^x\rangle \neq 0$. Indeed, this phase transition bears a resemblance to the superradiant quantum phase transition in the Dicke model with the addition of nontrivial spatial quantum fluctuations [36–39]. The emerging long-range ordering phase can be regarded as a delocalized superradiant phase since the excitations delocalize across the lattice [25,26,40].

It is important to highlight that the mean-field Hamiltonian \hat{H}_{MF} [Eq. (5)] exhibits different features from the mean-field Hamiltonian of the RLM in Ref. [25]. Due to the coupling between the photon field and the QTFL, the mean-field atomic transition energy zJm is dependent on both the photon frequency ω and the atom-photon coupling g , which cannot be initially determined, while in the RLM they are independent. Consequently, both the mean-field treatments and obtained results differ significantly from those of the RLM [25].

In this paper, we propose a perturbative method to determine the expectation value m self-consistently. In the critical region, the order parameter ψ is small and we can expand m in the order of ψ , i.e.

$$m = m_0 + m_2\psi^2 + \dots, \quad (6)$$

where m_0 and m_2 are the coefficients of the corresponding power of ψ and can be determined self-consistently. Note that all odd-order terms in the expansion Eq. (6) vanish because of the invariance of m under the global gauge transformation,

$$\psi \rightarrow -\psi, \quad \hat{b}_i \rightarrow -\hat{b}_i, \quad \hat{\sigma}_i^x \rightarrow -\hat{\sigma}_i^x. \quad (7)$$

Then, the mean-field Hamiltonian can be expressed as a sum over individual sites, $\hat{H}_{\text{MF}} = \sum_i \hat{h}_i^{\text{MF}}$, where the single site mean-field Hamiltonian \hat{h}_i^{MF} is expanded in the order of ψ as

$$\hat{h}_i^{\text{MF}} = \hat{H}_i^{\text{R}} - zt\psi(\hat{b}_i^\dagger + \hat{b}_i) + zJm_2\psi^2\hat{\sigma}_i^z + zt\psi^2 + \frac{zJm^2}{2} + O(\psi^4), \quad (8)$$

where the \hat{H}_i^{R} represents the Rabi model with the Hamiltonian

$$\hat{H}_i^{\text{R}} = zJm_0\hat{\sigma}_i^z + \omega\hat{b}_i^\dagger\hat{b}_i + g\hat{\sigma}_i^x(\hat{b}_i^\dagger + \hat{b}_i). \quad (9)$$

Around the critical point, the terms in \hat{h}_i^{MF} involving ψ can be treated perturbatively, resulting in an expansion of the ground

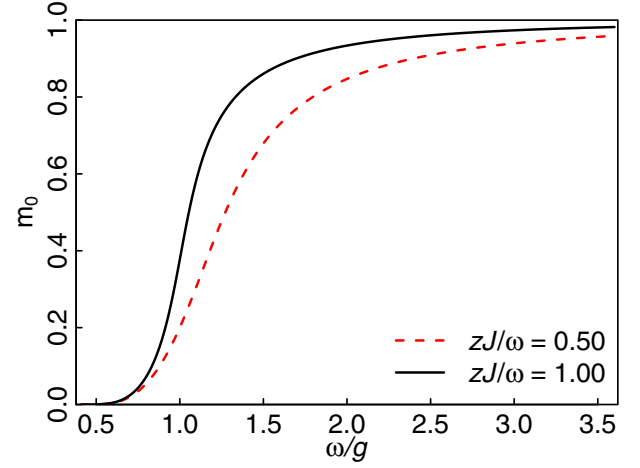


FIG. 2. The value of the self-consistent parameter m_0 at the critical point.

state $|G\rangle_i$ in powers of ψ as

$$|G\rangle_i = |0\rangle - z\psi \sum_{n \neq 0} |n\rangle \frac{\langle n | t(\hat{b}_i^\dagger + \hat{b}_i) | 0 \rangle}{E_0 - E_n} + O(\psi^2), \quad (10)$$

where $|n\rangle$ represents the exact n th eigenstate of the Rabi Hamiltonian \hat{H}_i^{R} , and E_n is the corresponding eigenenergy. The analytic solution of the Rabi model was found [41,42]. The self-consistent relation of the parameter m_0 can be obtained from the perturbative ground state $|G\rangle_i$ as

$$m_0 = -\langle 0 | \hat{\sigma}_i^z | 0 \rangle. \quad (11)$$

This equation can be solved iteratively to determine the value of m_0 accurately. Note that in the Rabi Hamiltonian \hat{H}_i^{R} [Eq. (9)], the atomic transition energy zJm_0 depends on both the coupling strength g and photon frequency ω , which is a primary difference from the counterpart mean-field Hamiltonian in the RLM [25]. To more intuitively demonstrate the differences, we presented the value of the self-consistent parameter m_0 at the critical point in Fig. 2. As the function of ω/g , m_0 varies greatly, indicating the significant influence on the phase boundary.

The parameters m_2 and the coefficient of higher power of ψ in Eq. (6) can be obtained self-consistently using an iterative approach similar to that used for m_0 . However, we only need to consider the self-consistent relation for m_0 , without explicitly treating the higher-order parameters. This is because, up to the order of ψ^2 , the ground-state energy E_g^{MF} in perturbation theory depends exclusively on m_0 . The expression of the perturbation ground-state energy in the powers of ψ is

$$\frac{E_g^{\text{MF}}}{N} = E_0 + zJ\frac{m_0^2}{2} + zt\psi^2 + z^2 \sum_{n \neq 0} \frac{\langle n | t(\hat{b}_i^\dagger + \hat{b}_i) | 0 \rangle^2}{E_0 - E_n} \psi^2 + O(\psi^4). \quad (12)$$

Due to the parity symmetry of \hat{H}_i^{R} , all odd-order terms also vanish in Eq. (12). In the spirit of Landau theory, the second-order terms being zero indicates a phase transition. Thus, the analytical expressions for the phase-transition boundary are

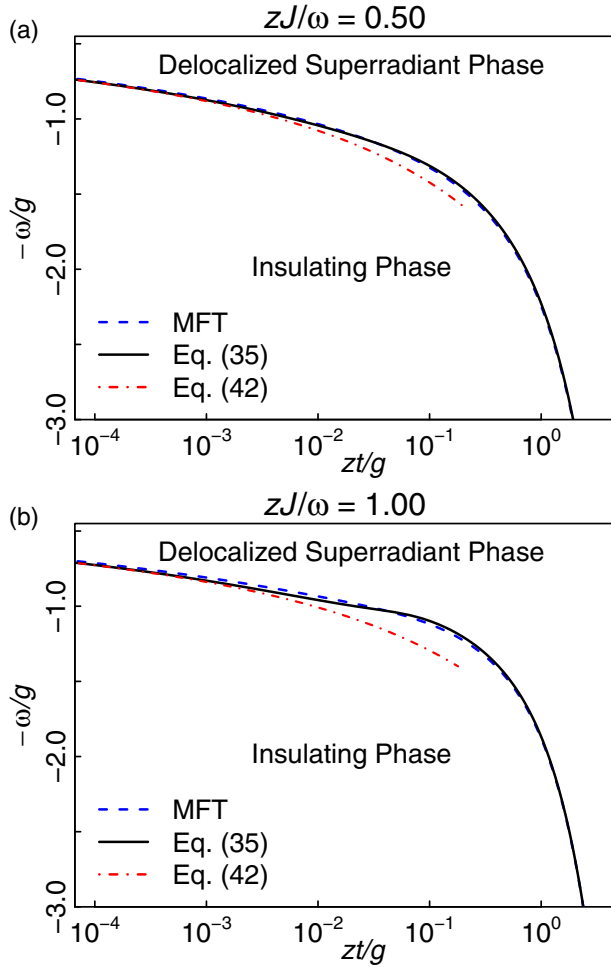


FIG. 3. The phase diagram of the two-dimensional IRLM obtained by the different approximation methods, in $(zt/g, \omega/g)$ plane: (a) for $zJ/\omega = 0.5$; (b) $zJ/\omega = 1$. The dashed line denotes the result of the mean-field theory (MFT) in Eq. (13), the solid line represents the result of the unitary transformation method in Eq. (24), and the dash-dotted line shows the result of the deep strong-coupling limit in Eq. (30). The horizontal axis is in a logarithmic scale.

obtained as

$$\frac{1}{zI_c} = - \sum_{n \neq 0} \frac{\langle n | (\hat{b}^\dagger + \hat{b}) | 0 \rangle^2}{E_0 - E_n}. \quad (13)$$

Since the effect of the dimension and the spatial lattice in the mean-field results is captured only by z , the phase boundary in Eq. (13) can be applied in the general lattice of arbitrary dimensions. Note that the eigenstate $|n\rangle$ differs from the counterpart in Ref. [25], as the atomic transition energy

$$\begin{aligned} \hat{H}'_0 = & -NV_0 + \sum_k \frac{\omega_k}{4} [\tau_k^2 |\hat{b}_{-k}^\dagger + \hat{b}_k|^2 - \tau_k^{-2} |\hat{b}_{-k}^\dagger - \hat{b}_k|^2 - 2] \\ & - \sum_{(i,j)} \hat{\sigma}_i^z \hat{\sigma}_j^z \sum_k \frac{J\beta_k \lambda_k^2}{4} (\hat{b}_k^\dagger \hat{b}_{-k}^\dagger + \hat{b}_k \hat{b}_{-k} - 2\hat{b}_k^\dagger \hat{b}_k) \\ & - \frac{(\kappa + \eta)J}{2} \sum_{(i,j)} \hat{\sigma}_i^z \hat{\sigma}_j^z + \frac{(\kappa - \eta)J}{2} \sum_{(i,j)} \hat{\sigma}_i^y \hat{\sigma}_j^y - \frac{1}{N} \sum_{i,j} \hat{\sigma}_i^x \hat{\sigma}_j^x \sum_k \left[\frac{g^2}{\omega_k} \xi_k (2 - \xi_k) - V_0 \right] e^{ik(r_i - r_j)}, \end{aligned} \quad (16)$$

zJm_0 depends on both the coupling strength g and photon frequency ω , in Eq. (9). For the Rabi model, the ground state is nondegenerate [41,42]. Due to $E_n > E_0$, the MFT always gives the positive critical hopping strength. Below the critical photon-hopping strength t_c , the value of $\psi = 0$ reveals the insulating phase. Above the critical photon-hopping strength t_c , the global \mathbb{Z}_2 parity symmetry \hat{P} is broken and the IRLM is in the delocalized superradiant phase with the nonzero order parameter $|\psi| > 0$. In Fig. 3, we present the mean-field phase diagram (dashed line) of the IRLM in the two-dimensional square lattice in $(zt/g, \omega/g)$ plane for $zJ/\omega = 0.5$ and $zJ/\omega = 1$. The results of the unitary transformation method and the DSC limit are shown in Sec. III.

Due to the lack of closed-form solutions in the Rabi model, it is hard to directly apply Eq. (13) to investigate the competition relation among the different energy scales (g , J , and t). Besides, the mean-field treatment cannot predict the low-lying excitation, which is important in low temperatures. In the next section, we use the unitary transformation to further reveal the property of the low-lying polaritonic excitations.

III. POLARITONIC EXCITATIONS AND BOSE-EINSTEIN CONDENSATION

The unitary transformation method has been used to successfully illustrate the phase transition and excitation behavior in the RLM [24,25]. In this section, we use the unitary transformation method to study the ground state and low-lying polaritonic excitation properties in the IRLM. The purpose of the transformation is to take into account the atom-photon correlation effect in the Rabi interaction. In the unitary transformation method, the displacement transformation \hat{S}_1 and the squeezing transformation \hat{S}_2 are performed to \hat{H}_{IR} , where

$$\hat{S}_1 = \frac{1}{\sqrt{N}} \sum_k \sum_i \frac{g \xi_k}{\omega_k} \hat{\sigma}_i^x (\hat{b}_{-k}^\dagger - \hat{b}_k) e^{-ikr_i}, \quad (14)$$

$$\hat{S}_2 = \frac{1}{2} \sum_k \ln(\tau_k) (\hat{b}_k \hat{b}_{-k} - \hat{b}_k^\dagger \hat{b}_{-k}^\dagger), \quad (15)$$

where \hat{b}_k is the Fourier form of the annihilation operator with frequency $\omega_k = \omega - zt\gamma_k$, and $\gamma_k = \sum_e \cos(\mathbf{k}e)/z$ is lattice dispersion (e is the unit lattice vector). The hopping coupling requires the \mathbf{k} -dependent displacement parameters ξ_k and the squeezing parameters τ_k , which will be determined later to eliminate the CRC terms. The unitary transformation performed on the Hamiltonian $\hat{H}' = e^{\hat{S}_2} e^{\hat{S}_1} \hat{H}_{\text{IR}} e^{-\hat{S}_1} e^{-\hat{S}_2}$ can be done straightforwardly to the end in Appendix A. The transformed Hamiltonian is divided into three parts, $\hat{H}' = \hat{H}'_0 + \hat{H}'_1 + \hat{H}'_2$, where

and \hat{H}'_1 [Eq. (A1)] and \hat{H}'_2 [Eq. (A2)] are presented in Appendix A. The parameter V_0 [Eq. (A4)] is subtracted to eliminate a constant self-interaction at the same site. For convenience, we introduce another two the parameters λ_k and β_k defined as

$$\lambda_k \equiv \frac{2g\xi_k}{\omega_k\tau_k}, \quad (17)$$

$$\beta_k \equiv \kappa + \eta + \gamma_k(\kappa - \eta), \quad (18)$$

where two photon-dressing parameters η and κ are defined as

$$\eta = \exp\left[-\frac{1}{N}\sum_k(1-\gamma_k)\lambda_k^2\right], \quad (19)$$

$$\kappa = \exp\left[-\frac{1}{N}\sum_k(1+\gamma_k)\lambda_k^2\right], \quad (20)$$

which arise from the rearrangement of the photon operators $\exp(\hat{X}_i - \hat{X}_j)$ and $\exp(\hat{X}_i + \hat{X}_j)$ into the normal ordering, respectively.

In the IRLM, the photon field inherently couples with the QTFI, and the competition arises among the photon-hopping coupling, the on-site Rabi interaction, and the intersite Ising interaction. The unitary transformation method reveals the various effects from this competition. Specifically, the Ising interaction induces two types of intersite interaction, namely, $\sigma_i^y\sigma_j^y$ and $\sigma_i^z\sigma_j^z$, with the renormalized interaction strengths $(\kappa - \eta)J/2$ and $(\kappa + \eta)J/2$, respectively. Additionally, the Rabi interaction induces another long-range interaction, i.e., $\sigma_i^x\sigma_j^x$. The photon-hopping coupling involves the \mathbf{k} -dependent displacement parameter ξ_k and the squeezing parameter τ_k . These \mathbf{k} -dependent parameters give rise to two different photon-dressing parameters η and κ . Consequently, all three types of intersite atom interactions (i.e., $\sigma_i^y\sigma_j^y$, $\sigma_i^z\sigma_j^z$, and $\sigma_i^x\sigma_j^x$) exhibit nonvanishing strength in the transformed Hamiltonian \hat{H}'_0 [Eq. (16)]. To the contrary, only a $\sigma_i^x\sigma_j^x$ term exists in the transformed Hamiltonian of the RLM [25]. Consequently, the different dependencies of the transformation parameters on the \mathbf{k} mode and a different quantum criticality are obtained.

A. Insulating phase

Through the Bogoliubov transformation and the linearized spin-wave approximation, we demonstrate the two-level atoms and photons are hybridized to form the polaritonic states in Appendix B. The unitary transformation treatment shares similarities with the approach outlined in Ref. [25], while the dependencies of the transformation parameters on the \mathbf{k} mode differs due to the addition of the intersite interactions (i.e., $\hat{\sigma}_i^y\hat{\sigma}_j^y$ and $\hat{\sigma}_i^z\hat{\sigma}_j^z$) and two types of the photon-dressing parameters κ and η . The transformed Hamiltonian \hat{H}' can be mapped to a diagonalized polariton model \hat{H}^I [see Eq. (B8)],

$$\hat{H}^I = E_g^I + \sum_{\mathbf{k}} E_{\Gamma}^{\pm}(\mathbf{k}) \hat{d}_{\pm\mathbf{k}}^{\dagger} \hat{d}_{\pm\mathbf{k}}, \quad (21)$$

where the two-branch excitation energy is

$$E_{\Gamma}^{\pm}(\mathbf{k}) = \frac{1}{2}(zJ\beta_k\rho_k^2 + \omega_k\tau_k^2) \pm \frac{1}{2}\sqrt{(zJ\beta_k\rho_k^2 - \omega_k\tau_k^2)^2 + 4g_{I\mathbf{k}}^2}. \quad (22)$$

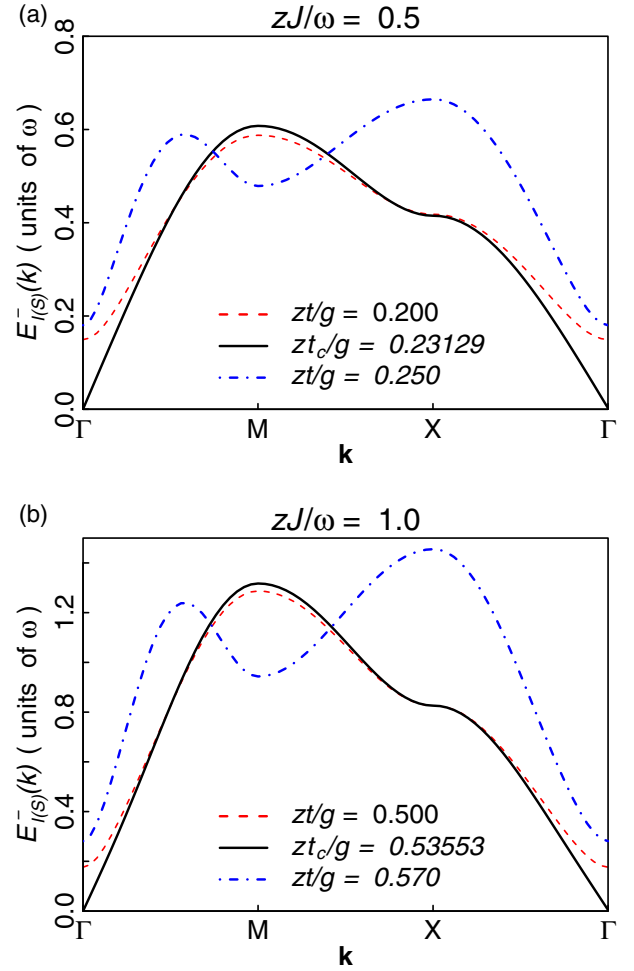


FIG. 4. The dispersion relation of the low-branch polaritonic excitations $E_{I(S)}^-(\mathbf{k})$ for the two-dimensional square lattice IRLM at $\omega = 1.5g$ around the critical points: (a) $zJ/\omega = 0.5$; (b) $zJ/\omega = 1$. Energies are in the units of ω .

In the insulating phase, the ground-state energy E_g^I [Eq. (B3)], the effective coupling strength $g_{I\mathbf{k}}$ [Eq. (B2)], the displacement function ξ_k [Eq. (B7)], the squeezing function τ_k [Eq. (B6)], and another Bogoliubov transformation parameter ρ_k [Eq. (B5)] are determined in Appendix B. Since the displacement transformation \hat{S}_1 and the squeezing transformation \hat{S}_2 are commutative with the parity operator \hat{P} , the insulating phase preserves the \mathbb{Z}_2 symmetry and is characterized by $\langle \hat{\sigma}_i^x \rangle = 0$ and $\langle \hat{b}_i \rangle = 0$.

The dispersion relation of the lower-energy branch $E_{\Gamma}^-(\mathbf{k})$ for the two-dimensional square lattice are plotted in Fig. 4(a) for $zJ/\omega = 0.5$ and Fig. 4(b) for $zJ/\omega = 1$ inside the insulating phase with $\omega = 1.5g$. The polaritonic excitation spectra are gapped cosine-like bands, and have their minima at the Γ point. As we show the case of $zJ/\omega = 0.5$ in Fig. 4(a), there exists a gap at $\mathbf{k} = 0$ in the insulating phase $zt/g = 0.200$. With the increase of zt/g , the gap comes to decrease. The gap $E_{\Gamma}^-(\mathbf{0})$ closes at the critical point, $zt_c/g = 0.23129$, with linear dispersion at small \mathbf{k} . Similar behavior is also found for the case $zt/\omega = 0.5$ in Fig. 4(b), where the gap $E_{\Gamma}^-(\mathbf{0})$ decreases with increasing of the hopping strength t , and eventually

disappears at the critical point $zt_c/g = 0.53553$. The gapped excitation energy ensures the stability of the insulating ground state.

We present the boundary of the phase transition. When the hopping strength t is above the critical point t_c , the polaritonic excitation energy $E_l^-(\mathbf{0})$ in Eq. (22) becomes negative. It indicates that the insulating ground state is no longer stable in this situation. In other words, the addition of more polaritons to the system always lowers the ground-state energy. Then macroscopic polaritons should occupy the ground state and the Bose-Einstein condensation of the polaritons emerges. Therefore, the condition for the presence of the stable insulating phase can be used as a criterion to determine the boundary of the phase transition,

$$2G_0 \leq zJ(\kappa + \eta), \quad (23)$$

where $G_0 = 2(g^2/\omega_0 - V_0)$.

The curve of the phase boundary is determined by the equation,

$$2G_0 = zJ(\kappa + \eta), \quad (24)$$

which can be solved numerically. In Fig. 3, we also plot the phase diagrams of the two-dimensional square lattice IRLM obtained by Eq. (24) in $(zt/g, \omega/g)$ plane. Since the phase diagrams from Eq. (24) are highly consistent with the MFT results, we confirm that the approximation used in the unitary transformation method is reasonable.

To get a better description of the phase transition, we further illustrate the influence of different energy scales on the phase transition boundary. In the unitary transformation method scheme, the photon-hopping coupling requires the \mathbf{k} -dependent displacement parameters ξ_k and the squeezing parameters τ_k . As a result, the Rabi interaction cooperates with the photon-hopping coupling inducing a nonvanishing long-range $\hat{\sigma}_i^x \hat{\sigma}_j^x$ interaction among the intersite atoms in the last term of \hat{H}'_0 [Eq. (16)], which favors the long-range ordering phase. On the contrary, the Ising interaction with coupling strength J prefers the insulating phase, which competes with the Rabi interaction and hopping coupling. The competition drives the system across the quantum phase transition. Consequently, the increase of the Ising interaction strength J requires the higher critical hopping coupling t_c to reach the long-range ordering phase, which is confirmed in Fig. 5, where the critical hopping strength zt_c/g is a monotonically increasing function with respect to the zJ/g .

B. Deep strong-coupling limit

Using the unitary transformation method, we take into account the atom-photon correlation in the Rabi interaction and obtain the ground state and the low-lying polaritonic excitation behavior. In the DSC limit, $g \gg \omega$, the equations (B6) and (B7) that determine the parameters of the unitary transformation can be solved and give $\tau_k = 1$ and $\xi_k = 1$. In this case, the ground state of the transformed Hamiltonian $\hat{H}' \simeq \hat{H}'_0 + \hat{H}'_1$ possesses the photon vacuum state, then it is reasonable to average the Hamiltonian \hat{H}' over the photon vacuum state $|\text{vac}\rangle$ as $\hat{H}_{XYZ} = \langle \text{vac} | \hat{H}' | \text{vac} \rangle$. As a result, the original IRLM Hamiltonian reduces to the quantum XYZ model [43,44] in

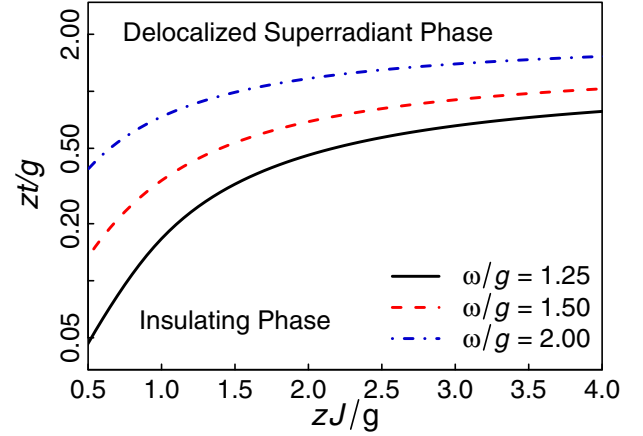


FIG. 5. The phase diagram of the two-dimensional square lattice IRLM in $(zt/g, zJ/g)$ plane with fixed $\omega/g = 1.25, 1.5, 2.00$. The vertical axis is in a logarithmic scale.

the weak hopping coupling case ($\omega \gg t$),

$$\begin{aligned} \hat{H}_{XYZ} = & \frac{Ng^2}{\omega} - \frac{(\kappa + \eta)J}{2} \sum_{(i,j)} \hat{\sigma}_i^z \hat{\sigma}_j^z - 2J \frac{g^2}{\omega^2} \sum_{(i,j)} \hat{\sigma}_i^x \hat{\sigma}_j^x \\ & + \frac{(\kappa - \eta)J}{2} \sum_{(i,j)} \hat{\sigma}_i^y \hat{\sigma}_j^y. \end{aligned} \quad (25)$$

Although the XYZ model is one of the most widely studied integrable models in one-dimensional chains [45,46], the phase diagram and the critical behavior of the XYZ model in the general lattice has not been fully investigated [47]. Following the approximation in Sec. III A, we derive the results of spin-wave theory for a general lattice [44]. After the linearized spin-wave approximation, \hat{H}_{XYZ} is approximated as

$$\begin{aligned} \hat{H}_{XYZ} \simeq & \frac{Ng^2}{\omega} - \frac{(\kappa + \eta)zJ}{4} + (\kappa + \eta)zJ \sum_k \hat{a}_k^\dagger \hat{a}_k \\ & - \frac{(\kappa - \eta)zJ}{4} \sum_k \gamma_k (\hat{a}_{-k}^\dagger - \hat{a}_k) (\hat{a}_k^\dagger - \hat{a}_{-k}) \\ & - zJ \frac{g^2}{\omega^2} \sum_k \gamma_k (\hat{a}_{-k}^\dagger + \hat{a}_k) (\hat{a}_k^\dagger + \hat{a}_{-k}), \end{aligned} \quad (26)$$

where the mean-field approximation is applied, $\sum_{(i,j)} \hat{\sigma}_i^z \hat{\sigma}_j^z \simeq z \sum_i \hat{\sigma}_i^z - \frac{z}{2}$. After a Bogoliubov transformation with the generator S_4 given by

$$\hat{S}_4 = \frac{1}{2} \sum_k \ln(\phi_k^{-1}) (\hat{a}_k \hat{a}_{-k} - \hat{a}_k^\dagger \hat{a}_{-k}^\dagger), \quad (27)$$

the XYZ model reduces to the free boson model as

$$\begin{aligned} e^{\hat{S}_4} \hat{H}_{XYZ} e^{-\hat{S}_4} = & -\frac{3(\kappa + \eta)zJN}{4} + \frac{Ng^2}{\omega} + \frac{1}{2} \sum_k zJ \beta_k \phi_k^2 \\ & + \sum_k zJ \beta_k \phi_k^2 \hat{a}_k^\dagger \hat{a}_k, \end{aligned} \quad (28)$$

where

$$\phi_k^2 = \sqrt{\frac{4}{zJ\beta_k} \left[\frac{(\kappa + \eta)zJ}{4} - \frac{g^2}{\omega^2} zJ\gamma_k \right]}. \quad (29)$$

The excitation energy spectrum is $zJ\beta_k\phi_k^2$, which has the minimum at $\mathbf{k} = 0$. The DSC limit results also give the gapped excitation energy in the insulating phase and the gap closes at the critical point t_c ,

$$t_c = \frac{\omega^2(\kappa + \eta)J}{g^2 4} \quad (30)$$

$$\simeq \frac{\omega^2 J}{2g^2} \exp\left(-\frac{4g^2}{\omega^2}\right) \cosh\left(\frac{4g^2}{\omega^2} \frac{2t_c}{\omega}\right). \quad (31)$$

Since the critical point t_c is always positive, it confirms that the photon-hopping coupling is necessary to induce the quantum phase transition in the IRLM.

The phase boundary obtained from the DSC limit in Eq. (30) is also plotted in Fig. 3. The results of the DSC limit are consistent with the general phase boundary in Eq. (24) in the case $g \gg \omega$. As the critical hopping strength $t_c \propto \frac{\omega^2 J}{2g^2} \exp(-\frac{4g^2}{\omega^2})$, even the weak hopping coupling can induce the quantum phase transition. As we show in Fig. 3(a), when the ratio $g/\omega \sim 1$, the critical hopping strength zt_c/g is on the order of 10^{-3} . Since the light-matter coupling has reached the DSC regime [15–17], this quantum phase transition could be observed in an experiment.

The DSC analysis reveals a feature of the IRLM. The competition among the photon-hopping coupling, the on-site Rabi interaction, and the intersite Ising interaction leads to the emergence of three distinct types of intersite atom interactions, i.e., $\sigma_i^x \sigma_j^x$, $\sigma_i^y \sigma_j^y$, and $\sigma_i^z \sigma_j^z$, with nonvanishing interaction strength, as shown in Eqs. (16) and (25). Thus, despite originating from the QTFI, the DSC analysis unveils that the IRLM belongs to the universality class of the XYZ model. This unique feature implies that the IRLM offers an alternative experimental setup for exploring the critical behavior of the XYZ model.

C. Delocalized superradiant phase

In the delocalized superradiant phase, we also apply the unitary transformation method to investigate the polaritonic excitations behavior near the critical point. When $2G_0 > zJ(\kappa + \eta)$, the ground state is characterized by the condensation of macroscopic polaritons, resulting in a coherent photon field and atomic polarization. To further approximately diagonalize the transformed Hamiltonian, we need to introduce a static displacement operator \hat{R} [Eq. (C1)] and a unitary rotation operator \hat{U} [Eq. (C2)], following the approach outlined in Ref. [25]. In Appendix C, the IRLM reduces to a diagonalized polariton model as \hat{H}^S [see Eq. (C13)]

$$\hat{H}^S = E_g^S + \sum_{\mathbf{k}} E_S^\pm(\mathbf{k}) \hat{p}_{\pm\mathbf{k}}^\dagger \hat{p}_{\pm\mathbf{k}}, \quad (32)$$

where the two-branch excitations energy is given by

$$E_S^\pm(\mathbf{k}) = \frac{1}{2} (W_{\mathbf{k}} \theta_{\mathbf{k}}^2 + \omega_{\mathbf{k}} \tau_{\mathbf{k}}^2) \pm \frac{1}{2} \sqrt{(W_{\mathbf{k}} \theta_{\mathbf{k}}^2 - \omega_{\mathbf{k}} \tau_{\mathbf{k}}^2)^2 + 4g_{S\mathbf{k}}^2}. \quad (33)$$

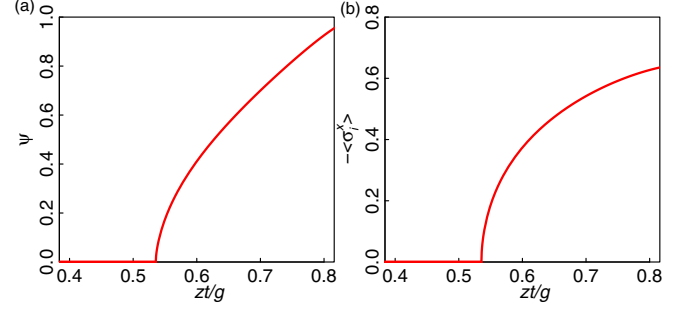


FIG. 6. (a) The order parameter $\psi = \langle \hat{b}_i \rangle$ with $\omega/g = 1.5$ and $\omega = zJ$. (b) The expectation value $-\langle \hat{\sigma}_i^x \rangle$ in the ground state with $\omega/g = 1.5$ and $\omega = zJ$. The critical point is $zt_c/g = 0.53553$.

In the delocalized superradiant phase, the ground-state energy E_g^S [Eq. (C5)], the effective coupling strength $g_{S\mathbf{k}}$ [Eq. (C4)], the parameter $W_{\mathbf{k}}$ [Eq. (C10)], the displacement function $\xi_{\mathbf{k}}$ [Eq. (C8)], the squeezing function $\tau_{\mathbf{k}}$ [Eq. (C9)], and the Bogoliubov transformation parameter $\theta_{\mathbf{k}}$ [Eq. (C7)] are determined in Appendix C.

To maintain the stability of the delocalized superradiant phase in the IRLM, the polariton excitations should have a positive-energy cost. Specifically, the lower-energy branch of polariton excitation energy $E_S^-(\mathbf{k})$ must be positive. Thus, the boundary for the stable delocalized superradiant phase can be expressed as

$$2G_0 \geq (\kappa + \eta)zJ. \quad (34)$$

which is in accordance with the phase boundary in the insulating phase [Eq. (24)].

In the delocalized superradiant phase, two typical low-branch polaritonic excitations $E_S^-(\mathbf{k})$ in the two-dimensional square lattice IRLM at $\omega = 1.5g$ are also plotted in Figs. 4(a) and 4(b), near the critical hopping strength t_c . In both cases, the polaritonic excitations have a positive gap in the delocalized superradiant phase.

In the delocalized superradiant phase, the \mathbb{Z}_2 symmetry with respect to the parity operator \hat{P} is broken, and the expectation of the $\langle \hat{\sigma}_i^x \rangle$ and the photonic annihilation operator $\psi = \langle \hat{b}_i \rangle$ in the ground state have nonvanishing values. The values of $\langle \hat{\sigma}_i^x \rangle$ and $\psi = \langle \hat{b}_i \rangle$ can be calculated by

$$\langle \hat{\sigma}_i^x \rangle = \frac{\sigma_0}{4} \frac{1}{N} \sum_{\mathbf{k}} (\theta_{\mathbf{k}}^{-2} + \theta_{\mathbf{k}}^2 - 2) - \sigma_0, \quad (35)$$

$$\psi = \frac{g\sigma_0}{\omega_0} - \frac{g\sigma_0\xi_0}{2\omega_0} \frac{1}{N} \sum_{\mathbf{k}} (\theta_{\mathbf{k}}^{-2} + \theta_{\mathbf{k}}^2 - 2). \quad (36)$$

The numerical results of ψ and $-\langle \hat{\sigma}_i^x \rangle$ as the functions of zt/g are presented in Fig. 6 with $\omega/g = 1.5$ and $\omega = zJ$.

IV. ABSENCE OF PHOTON-HOPPING COUPLING: $t = 0$

In this section, we consider the special situation $t = 0$. Then, the Hamiltonian of the IRLM [35] becomes

$$\hat{H}_{\text{IR}}^0 = \sum_i \omega \hat{b}_i^\dagger \hat{b}_i + \sum_i g \hat{\sigma}_i^x (\hat{b}_i^\dagger + \hat{b}_i) - J \sum_{(i,j)} \hat{\sigma}_i^z \hat{\sigma}_j^z, \quad (37)$$

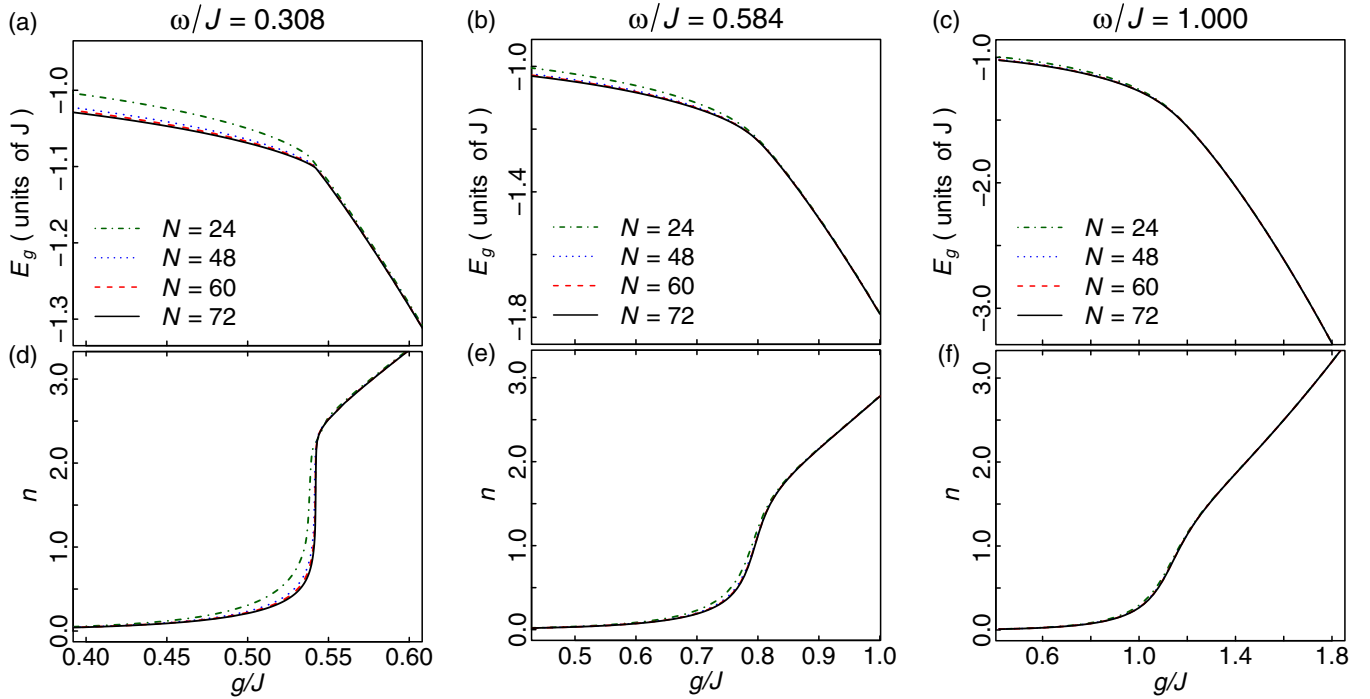


FIG. 7. The DMRG results of the one-dimensional hopping-absent IRLM \hat{H}_{IR}^0 with the chain length $N = 24, 48, 60, 72$ in the free boundary. The mean ground-state energy $E_g = \frac{1}{N} \langle G | \hat{H}_{\text{IR}}^0 | G \rangle$ as a function of the rescaled Rabi interaction strength g/J : (a) $\omega/J = 0.308$; (b) $\omega/J = 0.584$; (c) $\omega/J = 1$. The mean photon number $n = \frac{1}{N} \langle G | \hat{b}^\dagger \hat{b} | G \rangle$ as a function of the rescaled Rabi interaction strength g/J : (d) $\omega/J = 0.308$; (e) $\omega/J = 0.584$; (f) $\omega/J = 1$. Energies are in the units of J .

which still has the intersite coupling through the Ising interaction. The properties of the ground state will be investigated through the symmetry analysis and the numerical DMRG method. Despite the existence of the Ising interaction, the Hamiltonian \hat{H}_{IR}^0 does not exhibit a quantum phase transition. This unique characteristic reveals that even though the IRLM stems from the QTFI by substituting the transverse field with the quantized photon field, the photon field alone cannot serve as a global transverse field without the presence of hopping coupling.

A. Symmetry analysis

There exists a remarkable different symmetry property between this Hamiltonian \hat{H}_{IR}^0 without photon-hopping coupling and the original Hamiltonian \hat{H}_{IR} in Eq. (2). The Hamiltonian \hat{H}_{IR}^0 possesses a local \mathbb{Z}_2 symmetry with the parity operator $\hat{P}_i = \exp[i\pi(\hat{b}_i^\dagger \hat{b}_i + \hat{\sigma}_i^+ \hat{\sigma}_i^-)]$, since it is invariant under the transformation $\hat{P}_i^\dagger \hat{H}_{\text{IR}}^0 \hat{P}_i = \hat{H}_{\text{IR}}^0$. The photon-hopping coupling terms break the local symmetry \hat{P}_i but maintain the global symmetry with the parity operator $\hat{P} = \prod_i \hat{P}_i$. Besides, the Hamiltonian \hat{H}_{IR}^0 also possesses a global \mathbb{Z}_2 symmetry related to the parity operator $\hat{P} = \prod_i \hat{\sigma}_i^x$. On one hand, due to those two symmetries, it is easy to show the eigenstates are all doubly degenerate. According to Elitzur's theorem [48], i.e., the local symmetry \hat{P}_i cannot be spontaneously broken, the parity numbers with respect to \hat{P}_i are good quantum numbers. We denote the l th eigenstate of \hat{H}_{IR}^0 as $|\psi_l\rangle$, which satisfies $\hat{H}_{\text{IR}}^0 |\psi_l\rangle = E_l |\psi_l\rangle$ and $\hat{P}_i |\psi_l\rangle = p_i |\psi_l\rangle$ ($p_i = \pm 1$), where E_l is the eigenvalue of eigenstate $|\psi_l\rangle$. For each eigenstate $|\psi_l\rangle$, it has another eigenstate $|\psi_l'\rangle = \hat{P} |\psi_l\rangle$, where $|\psi_l\rangle$ and $|\psi_l'\rangle$

have the same eigenvalue E_l , but the opposite parity values of the operator \hat{P}_i . Then, all eigenstates are doubly degenerate. On the other hand, Elitzur's theorem requires the eigenstate to satisfy the parity \hat{P}_i , while $[\hat{P}_i, \hat{P}] \neq 0$. As a result, \hat{P} is always broken. Thus, the symmetry analysis indicates the quantum phase transition related to \hat{P} broken should be absent in the case of $t = 0$. It is a crossover behavior rather than a quantum phase transition with respect to the increasing of the Rabi interaction.

B. Density matrix renormalization group results

We use the DMRG algorithm [49,50] to further investigate the ground-state properties of the \hat{H}_{IR}^0 in a chain of N sites with the free boundary. The DMRG algorithm is implemented, utilizing the C++ version of the ITensor library [51], and the cutoff for the maximum Fock state of local photon number is set as $M_c = 50$, which is large enough to confirm that the DMRG algorithm converges. In Fig. 7, we show the mean ground-state energy $E_g = \frac{1}{N} \langle G | \hat{H}_{\text{IR}}^0 | G \rangle$ and the mean photon number $n = \frac{1}{N} \langle G | \hat{b}^\dagger \hat{b} | G \rangle$ as a function of rescaled coupling strength g/J with the chain length $N = 24, 48, 60, 72$. The results show that the curves of E_g and n almost collapse together for the $N \gtrsim 48$ in all the cases $J/\omega = 0.308$ [Figs. 7(a) and 7(d)], $J/\omega = 0.584$ [Figs. 7(b) and 7(e)], and $J/\omega = 1$ [Figs. 7(c) and 7(f)]. It means that the chain with $N = 72$ sites is large enough to describe the properties of the ground state in the thermodynamic limit. In Fig. 7, the DMRG results show that as the increase of Rabi interaction strength g/J , the ground-state energy decreases and the mean photon number increases gradually. Although the ascending slope of

the mean photon number becomes much steeper in the small ratio ω/J , neither nonanalytic nor discontinuous behaviors are presented in Fig. 7. Thus, the mean photon number should not be regarded as the order parameter, which is zero below the phase-transition point and has a finite value above the phase-transition point. Besides, the important feature of finite-size scaling behavior [52–54] for the second-order phase transition is also absent. Consequently, as the Rabi interaction strength g/J increases, it is more reasonable to regard the rapid growth of the photon number as a crossover behavior rather than a quantum phase transition.

V. CONCLUSION

In this work, we study the ground state and the spectra of low-lying excitations of the IRLM. The IRLM combines two paradigmatic models, the RLM from quantum optics and QTFI from condensed-matter physics, where the transverse field in the QTFI is replaced by the quantized photon field. Due to highly experimental achievement, the IRLM can be realized by the trapped ions [35] or superconducting qubits [55]. We expect that the IRLM can serve as the paradigmatic model to study light-matter coupling systems.

In the IRLM, the competition among the photon-hopping coupling, the intrasite Rabi interaction, and the Ising interaction drives the system across a quantum phase transition from the insulating phase to the delocalized superradiant phase. The mean-field treatment is applied to clarify the existence of a quantum phase transition, and the analytical expressions for the phase boundary are derived. By the unitary transformation method, the IRLM maps to the polariton model, and polaritonic excitations are explored beyond the mean-field approximation. In the weak hopping situation, the system is in the insulating phase with gapped polaritonic excitations. With the increase of the hopping strength until to the critical point t_c , the insulating ground state becomes no longer stable and Bose-Einstein condensation emerges. From the stability of the ground state, we obtain the analytical expression for the boundary of the phase transition, which is consistent with the MFT results. Above the critical point, macroscopic polaritons occupy the ground state, resulting in the coherent photon field and atomic polarization. The DSC analysis demonstrates that the critical hopping strength t_c exponentially decays, indicating the potential observability of the quantum phase transition in experimental settings. Moreover, the critical behavior of the IRLM is characterized by the universality class of the XYZ model.

Compared with the RLM in the previous paper Ref. [25], the primary difference between the two models is that, in the IRLM, the photon field inherently couples with the strongly correlated model, while in the RLM, the photon field only couples with a local two-level system. Due to their unique physics, the two models exhibit different interaction competitions and yield distinct results. In the IRLM, the Ising interaction and photon-hopping coupling terms couple

nearest-neighbor sites simultaneously. Within the mean-field theory framework, this gives rise to not only the order parameter $\psi \equiv \langle \hat{b}_j \rangle$ but also another self-consistent parameter $m \equiv -\langle \hat{\sigma}_i^z \rangle$. The value of m depends on both Ising interaction strength J and the atom-photon coupling strength g , leading to significant variations of m at the critical point, as observed in Fig. 2. Unlike in the IRLM, the self-consistent parameter $m \equiv -\langle \hat{\sigma}_i^z \rangle$ is absent in the RLM. As a result, the phase boundary [Eq. (13)] predicted by the MFT of the IRLM is significantly different from that of the RLM. In the IRLM, the competition arises among the photon-hopping coupling, the on-site Rabi interaction, and the intersite Ising interaction. The unitary transformation method results reveal that the competition leads to three types of nonvanishing intersite atom interactions (i.e., $\sigma_i^y \sigma_j^y$, $\sigma_i^z \sigma_j^z$, and $\sigma_i^x \sigma_j^x$) in the transformed Hamiltonian \hat{H}'_0 [Eq. (16)]. On the contrary, only a $\sigma_i^x \sigma_j^x$ term exists in the transformed Hamiltonian of the RLM [25]. The actually distinct obtained results between the IRLM and the RLM are not only reflected in the dependencies of the transformation parameters on the \mathbf{k} mode [Eqs. (B5), (B6), (B7), (C7), (C8), and (C9)], but also the emergence of different quantum criticality. DSC analysis unveils that the IRLM belongs to the universality class of the XYZ in Sec. III B, while the RLM falls into the Ising universality class Ref. [25].

The necessity of the photon-hopping coupling for inducing the quantum phase transition is further confirmed by considering the case of the hopping strength $t = 0$. Due to Elitzur's theorem, the global \mathbb{Z}_2 symmetry related to the parity operator $\hat{\mathcal{P}} = \prod_i \hat{\sigma}_i^x$ in the IRLM is always broken, and the quantum phase transition is absent. The DMRG also shows that the mean photon numbers as a function of the Rabi interaction g/J increase gradually. The corresponding process should be regarded as a crossover behavior rather than a quantum phase transition in the finite ratio J/ω . Therefore, our research has uncovered a feature in the IRLM. Despite the fact that the IRLM stems from the QTFI, we prove that the photon field alone cannot serve as a global transverse field without the presence of hopping coupling.

ACKNOWLEDGMENTS

This work is supported by the National Natural Science Foundation of China Grants No. 11947231, No. 11874260, and No. 11774226. H.Q. Lin acknowledges financial support from the National Natural Science Foundation of China under Grant No. 12088101.

APPENDIX A: THE TRANSFORMED HAMILTONIAN

The unitary transformation performed on Hamiltonian $\hat{H}' = e^{\hat{S}_2} e^{\hat{S}_1} \hat{H}_{\text{IR}} e^{-\hat{S}_1} e^{-\hat{S}_2}$ can be done straightforwardly to the end. The transformed Hamiltonian is divided into three parts, $\hat{H}' = \hat{H}'_0 + \hat{H}'_1 + \hat{H}'_2$, where \hat{H}'_0 is presented in main text in Eq. (16), and

$$\hat{H}'_1 = \frac{1}{\sqrt{N}} \sum_k \sum_i g(1 - \xi_k) \tau_k \hat{\sigma}_i^x (\hat{b}_{-k}^\dagger + \hat{b}_k) e^{-ikr_i} + J \sum_{(i,j),k} i \hat{\sigma}_i^y \hat{\sigma}_j^z \frac{\beta_k \lambda_k}{2\sqrt{N}} (\hat{b}_{-k}^\dagger - \hat{b}_k) e^{-ikr_i}, \quad (\text{A1})$$

$$\begin{aligned} \hat{H}'_2 = & J \sum_{(i,j)} \hat{\sigma}_i^y \hat{\sigma}_j^y \left[\sinh(\hat{X}_i) \sinh(\hat{X}_j) - \frac{\kappa - \eta}{2} \right] + 2J \sum_{(i,j)} i \hat{\sigma}_i^y \hat{\sigma}_j^z \left[\sinh(\hat{X}_i) \cosh(\hat{X}_j) - \sum_k \frac{\lambda_k \beta_k}{4\sqrt{N}} (\hat{b}_{-k}^\dagger - \hat{b}_k) e^{-ikr_i} \right] \\ & - J \sum_{(i,j)} \hat{\sigma}_i^z \hat{\sigma}_j^z \left[\cosh(\hat{X}_i) \cosh(\hat{X}_j) - \frac{\kappa + \eta}{2} - \sum_k \frac{\lambda_k^2 \beta_k}{4} (\hat{b}_k^\dagger \hat{b}_{-k}^\dagger + \hat{b}_k \hat{b}_{-k} - 2\hat{b}_k^\dagger \hat{b}_k) \right]. \end{aligned} \quad (\text{A2})$$

The operator \hat{X}_i and V_0 are introduced as

$$\hat{X}_i \equiv \frac{2}{\sqrt{N}} \sum_k \frac{g \xi_k}{\omega_k \tau_k} (\hat{b}_{-k}^\dagger - \hat{b}_k) e^{-ikr_i}, \quad (\text{A3})$$

$$V_0 \equiv \frac{1}{N} \sum_k \frac{g^2 \xi_k}{\omega_k} (2 - \xi_k). \quad (\text{A4})$$

As we have shown in Eqs. (16), (A1), and (A2), one and two-photon terms have been included in the \hat{H}'_0 and \hat{H}'_1 , and the parts that remained in the \hat{H}'_2 are the products of three or a higher number of photon operators in normal ordering with renormalized coupling strength. When we focus on the ground and low-lying excited states, it is reasonable to drop \hat{H}'_2 in the following calculation. It is worth emphasizing that the neglect of the \hat{H}'_2 does not mean that our result is valid only to the second order of g . It is obvious to see that the photon-dressing parameters η and κ , introduced in Eqs. (19) and (20), includes the infinite order of g . Thus, with the form of \hat{H}'_0 and \hat{H}'_1 , the strong-coupling effects on the ground and low-lying excited states can be explored to a satisfactory degree.

APPENDIX B: THE UNITARY TRANSFORMATION IN THE INSULATING PHASE

To simplify the transformed Hamiltonian $\hat{H}' \simeq \hat{H}'_0 + \hat{H}'_1$, the Pauli matrices in \hat{H}' are treated by the linearized spin-wave approximation as $\hat{\sigma}_i^z = 2\hat{a}_i^\dagger \hat{a}_i - 1$, $\hat{\sigma}_i^x = \hat{a}_i^\dagger + \hat{a}_i$, and $i\hat{\sigma}_i^y = \hat{a}_i^\dagger - \hat{a}_i$, with \hat{a}_i and \hat{a}_i^\dagger being bosonic operators [56]. Under this approximation, $\hat{\sigma}_i^z$ is well approximated as -1 , a constant, in the intersite interaction terms. The transformed Hamiltonian \hat{H}' ($\simeq \hat{H}'_0 + \hat{H}'_1$) can be diagonalized by further applying a Bogoliubov transformation as $\hat{H}^I = e^{\hat{S}_3} \hat{H}' e^{-\hat{S}_3}$,

$$\begin{aligned} \hat{H}^I = & E_g^I + \sum_k \omega_k \tau_k^2 \hat{b}_k^\dagger \hat{b}_k + \sum_k zJ \beta_k \rho_k^2 \hat{a}_k^\dagger \hat{a}_k \\ & + \sum_k g_{Ik} (\hat{b}_k^\dagger \hat{a}_k + \hat{b}_k \hat{a}_k^\dagger), \end{aligned} \quad (\text{B1})$$

where the effective coupling strength g_{Ik} between the atom and the photon is

$$g_{Ik} = 2g\tau_k(1 - \xi_k)\rho_k^{-1}, \quad (\text{B2})$$

and the ground-state energy of the insulating phase is given by

$$\begin{aligned} \frac{E_g^I}{N} = & -\frac{3(\kappa + \eta)zJ}{4} - NV_0 + \frac{1}{N} \sum_k \frac{\omega_k}{4} (\tau_k^2 + \tau_k^{-2} - 2) \\ & + \frac{1}{N} \sum_k \frac{zJ\beta_k}{2} \rho_k^2, \end{aligned} \quad (\text{B3})$$

The generator of the Bogoliubov transformation is

$$\hat{S}_3 = \frac{1}{2} \sum_k \ln(\rho_k^{-1}) (\hat{a}_k \hat{a}_{-k} - \hat{a}_k^\dagger \hat{a}_{-k}^\dagger), \quad (\text{B4})$$

with the parameter function ρ_k given by

$$\rho_k^2 = \tau_k^2 \sqrt{\frac{\kappa + \eta}{\beta_k} + \frac{4}{zJ\beta_k} \left(V_0 - \frac{g^2}{\omega_k} \right)}. \quad (\text{B5})$$

The squeezing function τ_k is given by

$$\tau_k^2 = \sqrt{1 + \frac{4zJg^2\beta_k\xi_k^2}{\omega_k^3}} \quad (\text{B6})$$

to eliminate the two-photon operators, and the parameter functions ξ_k is given by

$$\xi_k = \frac{\omega_k \tau_k^2}{\omega_k \tau_k^2 + zJ\beta_k \rho_k^2} \quad (\text{B7})$$

to eliminate the CRC terms in H^I .

By means of the linear transformation, the system reduces to a diagonalized polariton model:

$$\hat{H}^I = E_g^I + \sum_k E_I^\pm(\mathbf{k}) \hat{d}_{\pm\mathbf{k}}^\dagger \hat{d}_{\pm\mathbf{k}}, \quad (\text{B8})$$

where

$$\hat{d}_{-\mathbf{k}} = \cos \alpha \hat{a}_k - \sin \alpha \hat{b}_k, \quad (\text{B9})$$

$$\hat{d}_{+\mathbf{k}} = \sin \alpha \hat{a}_k + \cos \alpha \hat{b}_k, \quad (\text{B10})$$

with $\tan 2\alpha = 2g_{Ik}/(\omega_k \tau_k^2 - zJ\beta_k \rho_k^2)$.

APPENDIX C: THE UNITARY TRANSFORMATION IN THE DELOCALIZED SUPERRADIANT PHASE

In this Appendix, we reveal that the IRLM can be simplified to a polariton model in the delocalized superradiant phase. As the photon field becomes locally coherent and the atom is polarized, a static displacement of $\mathbf{k} = 0$ photon mode and a whole lattice rotation on the atom are required. We perform a displacement transformation \hat{R} and a rotation $\hat{U} = \prod_i \hat{U}_i$ on \hat{H}' as $\hat{U}^\dagger e^{\hat{R}} \hat{H}' e^{-\hat{R}} \hat{U}$. The displacement transformation \hat{R} is given by

$$\hat{R} = -\frac{\sqrt{N}g\sigma_0(1 - \xi_0)}{\omega_0 \tau_0} (\hat{b}_0^\dagger - \hat{b}_0), \quad (\text{C1})$$

where $\sigma_0^2 = 1 - [(\kappa + \eta)zJ]^2/(4G_0^2)$. The unitary matrix \hat{U}_i makes the Pauli matrices at every site i rotate as

$$\hat{U}_i^\dagger \left[\frac{(\kappa + \eta)zJ}{2} \hat{\sigma}_i^z + G_0 \sigma_0 \hat{\sigma}_i^x \right] \hat{U}_i = \frac{W}{2} \hat{\sigma}_i^z, \quad (\text{C2})$$

where $W^2 = 4(G_0\sigma_0)^2 + [(\kappa + \eta)zJ]^2$. Near the critical point, the mean-field approximation, i.e., $\sum_{(i,j)} \hat{\sigma}_i^z \hat{\sigma}_j^z \simeq z \sum_i \hat{\sigma}_i^z - \frac{z}{2}$, the spin-wave approximation, and a Bogoliubov transformation \hat{S}_4 are further applied to diagonalize the transformed Hamiltonian as $\hat{H}^S = e^{\hat{S}_5} \hat{U}^\dagger e^{\hat{R}} \hat{H}' e^{-\hat{R}} \hat{U} e^{-\hat{S}_5}$,

$$\hat{H}^S \simeq E_g^S + \sum_k \omega_k \tau_k^2 \hat{b}_k^\dagger \hat{b}_k + \sum_k W_k \theta_k^2 \hat{a}_k^\dagger \hat{a}_k - \sum_k g_{Sk} (\hat{b}_k^\dagger \hat{a}_k + \hat{b}_k \hat{a}_k^\dagger), \quad (\text{C3})$$

where the three-photon and higher-photon operators interactions are ignored, the effective coupling strength g_{Sk} between \hat{a}_k and \hat{b}_k is

$$g_{Sk} = 2(\kappa + \eta)zJg\tau_k(1 - \xi_k)/(W\theta_k), \quad (\text{C4})$$

and the corresponding ground-state energy of the delocalized superradiant phase is

$$E_g^S = N \frac{(\kappa + \eta)zJ}{4} - NW - NV_0 + \frac{NG_0\sigma_0^2}{2} + \sum_k \frac{\omega_k}{4} (\tau_k^2 + \tau_k^{-2} - 2) + \sum_k \frac{W_k \theta_k^2}{2}. \quad (\text{C5})$$

The generator of the Bogoliubov transformation is

$$\hat{S}_5 = \frac{1}{2} \sum_k \ln(\theta_k^{-1}) (\hat{a}_k \hat{a}_{-k} - \hat{a}_k^\dagger \hat{a}_{-k}^\dagger), \quad (\text{C6})$$

where the Bogoliubov parameter θ_k is given by

$$\theta_k^2 = \sqrt{\frac{W - \left[\frac{2(\kappa+\eta)zJ}{W}\right]^2 \left[\frac{g^2}{\omega_k} \xi_k (2 - \xi_k) - V_0\right]}{W_k}}. \quad (\text{C7})$$

The displacement parameter ξ_k , and the squeezing parameter τ_k are determined by

$$\xi_k = \frac{\omega_k \tau_k^2}{\omega_k \tau_k^2 + zJ\beta_k \theta_k^2}, \quad (\text{C8})$$

$$\tau_k^2 = \sqrt{1 + \frac{4zJ\beta_k g^2 \xi_k^2}{\omega_k^3} \left[\frac{(\kappa + \eta)zJ}{W}\right]^2}, \quad (\text{C9})$$

where

$$W_k = W + zJ(\kappa - \eta)\gamma(\mathbf{k}). \quad (\text{C10})$$

Using the linear transformation,

$$\hat{p}_{-k} = \cos \beta \hat{a}_k - \sin \beta \hat{b}_k, \quad (\text{C11})$$

$$\hat{p}_{+k} = \sin \beta \hat{a}_k + \cos \beta \hat{b}_k, \quad (\text{C12})$$

the IRLM reduces to a diagonalized polariton model,

$$\hat{H}^S = E_g^S + \sum_k E_S^\pm(\mathbf{k}) \hat{p}_{\pm k}^\dagger \hat{p}_{\pm k}, \quad (\text{C13})$$

where $\tan 2\beta = 2g_{Sk}/(\omega_k \tau_k^2 - W_k \theta_k^2)$. This linear transformation reveals the composite nature of the polaritons.

-
- [1] R. Hillenbrand, T. Taubner, and F. Keilmann, Phonon-enhanced light-matter interaction at the nanometre scale, *Nature (London)* **418**, 159 (2002).
- [2] N. Rivera and I. Kaminer, Light-matter interactions with photonic quasiparticles, *Nat. Rev. Phys.* **2**, 538 (2020).
- [3] R. Gutzler, M. Garg, C. R. Ast, K. Kuhnke, and K. Kern, Light-matter interaction at atomic scales, *Nat. Rev. Phys.* **3**, 441 (2021).
- [4] H. Mabuchi and A. Doherty, Cavity quantum electrodynamics: Coherence in context, *Science* **298**, 1372 (2002).
- [5] H. Walther, B. T. Varcoe, B.-G. Englert, and T. Becker, Cavity quantum electrodynamics, *Rep. Prog. Phys.* **69**, 1325 (2006).
- [6] I. I. Rabi, On the process of space quantization, *Phys. Rev.* **49**, 324 (1936).
- [7] A. Wallraff, D. I. Schuster, A. Blais, L. Frunzio, R. S. Huang, J. Majer, S. Kumar, S. M. Girvin, and R. J. Schoelkopf, Strong coupling of a single photon to a superconducting qubit using circuit quantum electrodynamics, *Nature (London)* **431**, 162 (2004).
- [8] M. M. Parish, Excitons in a new light, *Nat. Phys.* **17**, 16 (2020).
- [9] E. Jaynes and F. Cummings, Comparison of quantum and semiclassical radiation theories with application to the beam maser, *Proc. IEEE* **51**, 89 (1963).
- [10] T. Niemczyk, F. Deppe, H. Huebl, E. P. Menzel, F. Hocke, M. J. Schwarz, J. J. Garcia-Ripoll, D. Zueco, T. Hümmer, E. Solano, A. Marx, and R. Gross, Circuit quantum electrodynamics in the ultrastrong-coupling regime, *Nat. Phys.* **6**, 772 (2010).
- [11] P. Forn-Díaz, L. Lamata, E. Rico, J. Kono, and E. Solano, Ultrastrong coupling regimes of light-matter interaction, *Rev. Mod. Phys.* **91**, 025005 (2019).
- [12] A. Frisk Kockum, A. Miranowicz, S. De Liberato, S. Savasta, and F. Nori, Ultrastrong coupling between light and matter, *Nat. Rev. Phys.* **1**, 19 (2019).
- [13] P. Forn-Díaz, J. Lisenfeld, D. Marcos, J. J. García-Ripoll, E. Solano, C. J. P. M. Harmans, and J. E. Mooij, Observation of the Bloch-Siegert Shift in a Qubit-Oscillator System in the Ultrastrong Coupling Regime, *Phys. Rev. Lett.* **105**, 237001 (2010).
- [14] Z. Lü and H. Zheng, Effects of counter-rotating interaction on driven tunneling dynamics: Coherent destruction of tunneling and Bloch-Siegert shift, *Phys. Rev. A* **86**, 023831 (2012).
- [15] J. Casanova, G. Romero, I. Lizuain, J. J. García-Ripoll, and E. Solano, Deep Strong Coupling Regime of the Jaynes-Cummings Model, *Phys. Rev. Lett.* **105**, 263603 (2010).
- [16] A. Crespi, S. Longhi, and R. Osellame, Photonic Realization of the Quantum Rabi Model, *Phys. Rev. Lett.* **108**, 163601 (2012).
- [17] F. Yoshihara, T. Fuse, S. Ashhab, K. Kakuyanagi, S. Saito, and K. Semba, Superconducting qubit-oscillator circuit beyond the ultrastrong-coupling regime, *Nat. Phys.* **13**, 44 (2017).
- [18] J. M. Raimond, M. Brune, and S. Haroche, Manipulating quantum entanglement with atoms and photons in a cavity, *Rev. Mod. Phys.* **73**, 565 (2001).
- [19] A. Zeilinger, Experiment and the foundations of quantum physics, *Rev. Mod. Phys.* **71**, S288 (1999).

- [20] D. Porras and J. I. Cirac, Bose-Einstein Condensation and Strong-Correlation Behavior of Phonons in Ion Traps, *Phys. Rev. Lett.* **93**, 263602 (2004).
- [21] C. Shen, Z. Zhang, and L.-M. Duan, Scalable Implementation of Boson Sampling with Trapped Ions, *Phys. Rev. Lett.* **112**, 050504 (2014).
- [22] S. Debnath, N. M. Linke, S.-T. Wang, C. Figgatt, K. A. Landsman, L.-M. Duan, and C. Monroe, Observation of Hopping and Blockade of Bosons in a Trapped Ion Spin Chain, *Phys. Rev. Lett.* **120**, 073001 (2018).
- [23] Q.-X. Mei, B.-W. Li, Y.-K. Wu, M.-L. Cai, Y. Wang, L. Yao, Z.-C. Zhou, and L.-M. Duan, Experimental Realization of the Rabi-Hubbard Model with Trapped Ions, *Phys. Rev. Lett.* **128**, 160504 (2022).
- [24] H. Zheng and Y. Takada, Importance of counter-rotating coupling in the superfluid-to-Mott-insulator quantum phase transition of light in the Jaynes-Cummings lattice, *Phys. Rev. A* **84**, 043819 (2011).
- [25] G. Hu, Z. Lü, H. Lin, and H. Zheng, Polaritonic excitations and Bose-Einstein condensation in the Rabi lattice model, *Phys. Rev. A* **105**, 043710 (2022).
- [26] M. Schiró, M. Bordyuh, B. Öztop, and H. E. Türeci, Phase Transition of Light in Cavity QED Lattices, *Phys. Rev. Lett.* **109**, 053601 (2012).
- [27] A. D. Greentree, C. Tahan, J. H. Cole, and L. C. L. Hollenberg, Quantum phase transitions of light, *Nat. Phys.* **2**, 856 (2006).
- [28] J. Koch and K. Le Hur, Superfluid-Mott-insulator transition of light in the Jaynes-Cummings lattice, *Phys. Rev. A* **80**, 023811 (2009).
- [29] J. Zhao and M.-J. Hwang, Frustrated Superradiant Phase Transition, *Phys. Rev. Lett.* **128**, 163601 (2022).
- [30] Y.-Y. Zhang, Z.-X. Hu, L. Fu, H.-G. Luo, H. Pu, and X.-F. Zhang, Quantum Phases in a Quantum Rabi Triangle, *Phys. Rev. Lett.* **127**, 063602 (2021).
- [31] D. Fallas Padilla, H. Pu, G.-J. Cheng, and Y.-Y. Zhang, Understanding the Quantum Rabi Ring Using Analogies to Quantum Magnetism, *Phys. Rev. Lett.* **129**, 183602 (2022).
- [32] J. Zhao and M.-J. Hwang, Anomalous multicritical phenomena and frustration induced by synthetic magnetic fields, [arXiv:2208.02268](https://arxiv.org/abs/2208.02268).
- [33] P. Pfeuty, The one-dimensional Ising model with a transverse field, *Ann. Phys.* **57**, 79 (1970).
- [34] D. Porras and J. I. Cirac, Effective Quantum Spin Systems with Trapped Ions, *Phys. Rev. Lett.* **92**, 207901 (2004).
- [35] P. Nevado and D. Porras, Rabi lattice models with discrete gauge symmetry: Phase diagram and implementation in trapped-ion quantum simulators, *Phys. Rev. A* **92**, 013624 (2015).
- [36] C. Emary and T. Brandes, Chaos and the quantum phase transition in the Dicke model, *Phys. Rev. E* **67**, 066203 (2003).
- [37] C. Emary and T. Brandes, Quantum Chaos Triggered by Precursors of a Quantum Phase Transition: The Dicke Model, *Phys. Rev. Lett.* **90**, 044101 (2003).
- [38] P. Nataf and C. Ciuti, No-go theorem for superradiant quantum phase transitions in cavity QED and counter-example in circuit QED, *Nat. Commun.* **1**, 72 (2010).
- [39] M. Liu, S. Chesi, Z.-J. Ying, X. Chen, H.-G. Luo, and H.-Q. Lin, Universal Scaling and Critical Exponents of the Anisotropic Quantum Rabi Model, *Phys. Rev. Lett.* **119**, 220601 (2017).
- [40] S. Cui, F. Hébert, B. Grémaud, V. G. Rousseau, W. Guo, and G. G. Batrouni, Two-photon Rabi-Hubbard and Jaynes-Cummings-Hubbard models: Photon-pair superradiance, Mott insulator, and normal phases, *Phys. Rev. A* **100**, 033608 (2019).
- [41] D. Braak, Integrability of the Rabi Model, *Phys. Rev. Lett.* **107**, 100401 (2011).
- [42] Q.-H. Chen, C. Wang, S. He, T. Liu, and K.-L. Wang, Exact solvability of the quantum Rabi model using Bogoliubov operators, *Phys. Rev. A* **86**, 023822 (2012).
- [43] R. J. Baxter, *Exactly Solved Models in Statistical Mechanics* (Academic Press, 1982).
- [44] E. Manousakis, The spin- $\frac{1}{2}$ Heisenberg antiferromagnet on a square lattice and its application to the cuprous oxides, *Rev. Mod. Phys.* **63**, 1 (1991).
- [45] M. Takahashi, *Thermodynamics of One-Dimensional Solvable Models* (Cambridge University Press, 1999).
- [46] E. Ercolessi, S. Evangelisti, F. Franchini, and F. Ravanini, Essential singularity in the Renyi entanglement entropy of the one-dimensional XYZ spin- $\frac{1}{2}$ chain, *Phys. Rev. B* **83**, 012402 (2011).
- [47] J. Jin, W.-B. He, F. Iemini, D. Ferreira, Y.-D. Wang, S. Chesi, and R. Fazio, Determination of the critical exponents in dissipative phase transitions: Coherent anomaly approach, *Phys. Rev. B* **104**, 214301 (2021).
- [48] J. B. Kogut, An introduction to lattice gauge theory and spin systems, *Rev. Mod. Phys.* **51**, 659 (1979).
- [49] S. R. White, Density Matrix Formulation for Quantum Renormalization Groups, *Phys. Rev. Lett.* **69**, 2863 (1992).
- [50] S. R. White, Density-matrix algorithms for quantum renormalization groups, *Phys. Rev. B* **48**, 10345 (1993).
- [51] M. Fishman, S. R. White, and E. M. Stoudenmire, The ITensor software library for tensor network calculations, *SciPost Phys. Codebases* **4** (2022).
- [52] V. Privman and M. E. Fisher, Universal critical amplitudes in finite-size scaling, *Phys. Rev. B* **30**, 322 (1984).
- [53] X. Zhang, G. Hu, Y. Zhang, X. Li, and X. Chen, Finite-size scaling of correlation functions in finite systems, *Sci. China Phys. Mech. Astron.* **61**, 120511 (2018).
- [54] G. Hu, T. Liu, M. Liu, W. Chen, and X. Chen, Condensation of eigen microstate in statistical ensemble and phase transition, *Sci. China Phys. Mech. Astron.* **62**, 990511 (2019).
- [55] A. A. Houck, H. E. Türeci, and J. Koch, On-chip quantum simulation with superconducting circuits, *Nat. Phys.* **8**, 292 (2012).
- [56] Mattis and C. Daniel, *The Theory of Magnetism I Statics and Dynamics* (Springer-Verlag, 1981).